

# The COMMD Family Regulates Plasma LDL Levels and Attenuates Atherosclerosis Through Stabilizing the CCC Complex in Endosomal LDLR Trafficking

Alina Fedoseienko,\* Melinde Wijers,\* Justina C. Wolters, Daphne Dekker, Marieke Smit, Nicolette Huijkman, Niels Kloosterhuis, Helene Klug, Aloys Schepers, Ko Willems van Dijk, Johannes H.M. Levels, Daniel D. Billadeau, Marten H. Hofker,† Jan van Deursen, Marit Westerterp, Ezra Burstein, Jan Albert Kuivenhoven, Bart van de Sluis

**Rationale:** COMMD (copper metabolism MURR1 domain)-containing proteins are a part of the CCC (COMMD–CCDC22 [coiled-coil domain containing 22]–CCDC93 [coiled-coil domain containing 93]) complex facilitating endosomal trafficking of cell surface receptors. Hepatic COMMD1 inactivation decreases CCDC22 and CCDC93 protein levels, impairs the recycling of the LDLR (low-density lipoprotein receptor), and increases plasma low-density lipoprotein cholesterol levels in mice. However, whether any of the other COMMD members function similarly as COMMD1 and whether perturbation in the CCC complex promotes atherogenesis remain unclear.

**Objective:** The main aim of this study is to unravel the contribution of evolutionarily conserved COMMD proteins to plasma lipoprotein levels and atherogenesis.

**Methods and Results:** Using liver-specific *Commd1*, *Commd6*, or *Commd9* knockout mice, we investigated the relation between the COMMD proteins in the regulation of plasma cholesterol levels. Combining biochemical and quantitative targeted proteomic approaches, we found that hepatic COMMD1, COMMD6, or COMMD9 deficiency resulted in massive reduction in the protein levels of all 10 COMMDs. This decrease in COMMD protein levels coincided with destabilizing of the core (CCDC22, CCDC93, and chromosome 16 open reading frame 62 [C16orf62]) of the CCC complex, reduced cell surface levels of LDLR and LRP1 (LDLR-related protein 1), followed by increased plasma low-density lipoprotein cholesterol levels. To assess the direct contribution of the CCC core in the regulation of plasma cholesterol levels, *Ccdc22* was deleted in mouse livers via CRISPR/Cas9-mediated somatic gene editing. CCDC22 deficiency also destabilized the complete CCC complex and resulted in elevated plasma low-density lipoprotein cholesterol levels. Finally, we found that hepatic disruption of the CCC complex exacerbates dyslipidemia and atherosclerosis in ApoE3\*Leiden mice.

**Conclusions:** Collectively, these findings demonstrate a strong interrelationship between COMMD proteins and the core of the CCC complex in endosomal LDLR trafficking. Hepatic disruption of either of these CCC components causes hypercholesterolemia and exacerbates atherosclerosis. Our results indicate that not only COMMD1 but all other COMMDs and CCC components may be potential targets for modulating plasma lipid levels in humans. (*Circ Res.* 2018;122:1648-1660. DOI: 10.1161/CIRCRESAHA.117.312004.)

**Key Words:** atherosclerosis ■ endosome ■ hypercholesterolemia ■ liver ■ mice, transgenic

Clearing circulating atherogenic low-density lipoprotein (LDL) cholesterol is highly dependent on the LDLR (LDL receptor) in hepatocytes.<sup>1,2</sup> LDL binds to LDLR at the cell surface,

and the LDL–LDLR complex is endocytosed via clathrin-coated pits. On entering the endosomal network, LDLR is subjected to 1 of 2 fates decisions, either LDLR is sorted into the lysosome for

Original received September 5, 2017; revision received March 3, 2018; accepted March 13, 2018. In February 2018, the average time from submission to first decision for all original research papers submitted to *Circulation Research* was 12 days.

From the Molecular Genetics Section, Department of Pediatrics (A.F., M. Wijers, J.C.W., D.D., M.S., N.H., N.K., M.H.H., M. Westerterp, J.A.K., B.v.d.S.) and iPSC/CRISPR Center Groningen (B.v.d.S.), University Medical Center Groningen, University of Groningen, The Netherlands; PolyQuant GmbH, Bad Abbach, Germany (H.K.); Monoclonal Antibody Core Facility and Research Group, Institute for Diabetes and Obesity, Helmholtz Zentrum, München, Germany (A.S.); Department of Human Genetics (K.W.v.D.) and Department of Medicine (K.W.v.D.), Division of Endocrinology, Leiden University Medical Center, The Netherlands; Department of Vascular and Experimental Vascular Medicine, Academic Medical Center, University of Amsterdam, The Netherlands (J.H.M.L.); Division of Oncology Research, Department of Immunology and Biochemistry (D.D.B.), Department of Pediatrics and Adolescent Medicine, Mayo Clinic College of Medicine (J.v.D.), and Department of Biochemistry and Molecular Biology, Mayo Clinic College of Medicine (J.v.D.), Mayo Clinic, Rochester, MN; and University of Texas Southwestern Medical Center, Dallas (E.B.).

\*A.F. and M.W. contributed equally to this article.

†Deceased.

The online-only Data Supplement is available with this article at <http://circres.ahajournals.org/lookup/suppl/doi:10.1161/CIRCRESAHA.117.312004/-/DC1>.

Correspondence to Bart van de Sluis, Molecular Genetics Section, Department of Pediatrics, University of Groningen, University Medical Center Groningen, Antonius Deusinglaan 1, Groningen, The Netherlands. E-mail [a.j.a.van.de.sluis@umcg.nl](mailto:a.j.a.van.de.sluis@umcg.nl)

© 2018 American Heart Association, Inc.

*Circulation Research* is available at <http://circres.ahajournals.org>

DOI: 10.1161/CIRCRESAHA.117.312004

## Novelty and Significance

### What Is Known?

- The COMMD (copper metabolism Murr1 domain) family member COMMD1 participates in the CCC (COMMD–CCDC22–CCDC93) complex to facilitate endosomal trafficking of several transmembrane proteins, including the LDLR (low-density lipoprotein receptor).
- Studies in mice and dogs showed that hepatic COMMD1 deficiency increases plasma low-density lipoprotein cholesterol levels because of impaired endosomal LDLR transport, resulting in reduced LDLR levels at the cell surface.
- Hepatic COMMD1 deficiency reduces the protein expression of CCDC22 and CCDC93, and all 10 members of the COMMD protein family can interact with CCDC22, a protein that when mutated causes X-linked intellectual disability, a severe developmental disorder accompanied by hypercholesterolemia.

### What New Information Does This Article Contribute?

- Using liver-specific knockout mice for *Commd1*, *Commd6*, *Commd9*, and *Ccdc22*, we show that the integrity of the CCC complex and the protein stability of all members of the COMMD family are dependent on each other and that inactivation of the CCC complex in mouse livers leads to reduced cell surface levels of LDLR and LRP1 (LDLR-related protein 1), accompanied by increased plasma low-density lipoprotein cholesterol levels.
- The CCC complex facilitates endosomal trafficking of LDLR and LRP1.
- Hepatic inactivation of the CCC complex accelerates atherosclerosis in a mouse model with a human-like lipoprotein profile. Overall, our studies suggest that the endosomal trafficking of LDLR and LRP1 in clearing ApoB-containing particles are dependent on the CCC complex

and that the integrity of the CCC complex relies on the expression of all members of the COMMD family.

LDLR is a pivotal receptor in clearing plasma low-density lipoprotein cholesterol, and an impaired function of LDLR causes hypercholesterolemia and increased cardiovascular disease risk. The intracellular route of LDLR has been well established, but the mechanisms by which intracellular LDLR trafficking is orchestrated remain unclear. Mutations in the gene encoding for the CCC complex component CCDC22 cause the severe developmental disorder X-linked intellectual disability in humans. In this study, we examined the contribution of other COMMD proteins to plasma lipoprotein levels and atherogenesis. We found that the integrity of the CCC complex is not exclusively controlled by COMMD1 but by numerous members of the COMMD family. Furthermore, we showed that the stability of the COMMDs in hepatocytes relies on the CCC core component CCDC22, indicating a strong interrelation between the COMMD family and the core of the CCC complex. In addition, we found that not only the surface levels of LDLR are affected by CCC inactivation but also the surface levels of LRP1, implying that the CCC complex facilitates the endosomal trafficking of several members of the LDLR family. These reduced surface levels of LDLR and LRP1 eventually resulted in increased plasma ApoB-containing particles and accelerated atherosclerosis in mice. This study assigns a large number of candidate genes controlling plasma low-density lipoprotein cholesterol levels; however, whether plasma cholesterol levels and cardiovascular disease risk in humans can be explained by genetic variants in these genes needs to be evaluated.

### Nonstandard Abbreviations and Acronyms

<b>Apo</b>	apolipoprotein
<b>ATP7A</b>	ATPase copper transporting $\alpha$
<b>ATP7B</b>	ATPase copper transporting $\beta$
<b>C16orf62</b>	chromosome 16 open reading frame 62
<b>CCC</b>	COMMD–CCDC22–CCDC93
<b>CCDC22</b>	coiled-coil domain containing 22
<b>CCDC93</b>	coiled-coil domain containing 93
<b>COMMD</b>	copper metabolism MURR1 domain
<b>HFC</b>	high-fat high-cholesterol
<b>IDOL</b>	inducible degrader of the LDLR
<b>LDL</b>	low-density lipoprotein
<b>LDLR</b>	low-density lipoprotein receptor
<b>LRP1</b>	LDLR-related protein 1
<b>PCSK9</b>	proprotein convertase subtilisin/kexin type 9
<b>SNX17</b>	sortin nexin 17
<b>TC</b>	total cholesterol
<b>WASH</b>	Wiskott–Aldrich syndrome protein and SCAR homologue
<b>WT</b>	wild type

proteolysis or LDLR is reused and is recycled back to cell surface to take up the next cargo.<sup>3,4</sup> In the recent years, several proteins, such as PCSK9 (proprotein convertase subtilisin/kexin type 9) and IDOL (inducible degrader of the LDLR),<sup>5–7</sup> have been identified that avert the reuse of LDLR through directing LDLR to the

### Editorial, see p 1629

lysosomes, but the mechanism preventing the lysosomal fate and directing LDLR back to the cell surface is still not fully elucidated.

We recently uncovered the COMMD1 (copper metabolism MURR1 domain 1) as a novel factor in endosomal LDLR trafficking.<sup>8</sup> Loss of hepatic COMMD1 impairs the endocytic LDLR recycling, which subsequently results in increased levels of plasma LDL cholesterol in dogs and mice.<sup>8</sup> In addition to LDLR, COMMD1 also facilitates the endosomal trafficking of other receptors, such as the copper transporting protein ATP7A (ATPase copper transporting  $\alpha$ ) and ATP7B (ATPase copper transporting  $\beta$ ), to maintain copper homeostasis.<sup>9–11</sup> COMMD1 is assembled into the CCC (COMMD–CCDC22 [coiled-coil domain containing 22]–CCDC93 [coiled-coil domain containing 93]) complex together with chromosome 16 open reading frame 62 (C16orf62) and the coiled-coil proteins CCDC22 and CCDC93.<sup>9</sup> The CCC complex localizes to endosomes through physical association with the WASH (Wiskott–Aldrich syndrome protein and SCAR homologue) complex.<sup>9</sup> The recruitment of the CCC and WASH complexes to the endosomes is dependent on the retromer subunit VPS35.<sup>8,9,12</sup> WASH activates the Arp2/3 (actin-related protein 2/3) complex to deposit branched actin filaments on endosomes, which is essential for the architecture of the endosomal and lysosomal network and endosomal receptor trafficking.<sup>12–14</sup> The exact function of the CCC complex within the endosomal sorting

process is still unknown, but it is hypothesized to coordinate selective endosomal receptor trafficking.

COMMD1 belongs to the COMMD family, which consists of 10 members, each characterized by a carboxyl-terminal COMM (copper metabolism MURR1) domain, which mediates physical interaction with other COMMD proteins.<sup>15</sup> COMMD proteins are ubiquitously expressed and are conserved throughout evolution from lower organisms to higher vertebrates.<sup>15,16</sup> The COMMD proteins have a vital role in mouse embryonic development, as *Commd1*, *Commd6*, *Commd9*, or *Commd10* knockout mice are embryonically lethal<sup>17–20</sup> and die at different stages of embryogenesis, suggesting nonredundant functions of COMMD proteins during development. Although several studies have shown that the 10 COMMD proteins exist in large macromolecular complexes containing the CCC core components CCDC22, CCDC93, and C16orf62,<sup>9,18,21,22</sup> their role in the regulation of plasma cholesterol levels and atherogenesis has yet to be determined.

This study provides novel insights into the molecular organization of the endosomal sorting machinery in the coordination of intracellular trafficking of members of the LDLR family, such as LDLR and LRP1 (LDLR-related protein 1) and imply that all 10 COMMD proteins and the CCC core components may be potential targets modulating plasma lipid levels in humans.

## Methods

The authors declare that all supporting data are available within the article (and its [Online Data Supplement](#)).

A brief description of the methods is provided below. For a detailed description of the methods, please refer to the [online Data supplement](#).

### Animals

All animal studies were approved by the Institutional Animal Care and Use Committee, University of Groningen (Groningen, the Netherlands). Detailed description of the different mouse models can be found in the [Online Data Supplement](#).

### Hepatic Lipid Extraction

Lipid was extracted from liver homogenates and prepared as 15% (wt/vol) solutions in PBS, as previously described.<sup>23</sup> Samples were used to determine total cholesterol and triglyceride content.

### Fast-Performance Liquid Chromatography

Plasma samples of each group of mice were pooled and fractionated by fast-performance liquid chromatography as previously described,<sup>24</sup> with minor modifications. In brief, the system contained a PU-980 ternary pump with an LG-980-02 linear degasser and a UV-975 UV/VIS detector (Jasco, Tokyo). EDTA plasma was diluted 1:1 with Tris-buffered saline, and 300  $\mu$ L sample/buffer mixture was loaded onto a Superose 6 HR 10/300 column (GE Healthcare, Lifesciences Division, Diegem) for lipoprotein separation at a flow rate of 0.5 mL/min. Total cholesterol and triglyceride content of the fractions was determined as described above.

### Cholesterol and Triglyceride Analysis in Plasma and Liver Homogenates

Total cholesterol (TC) levels were determined using colorimetric assays (11489232; Roche) with cholesterol standard FS (DiaSys Diagnostic Systems GmbH) as a reference. Triglyceride levels were measured using Trig/GB kit (1187771; Roche) with Roche Precimat Glycerol standard (16658800) as a reference.

### Cell Lines

HEK293T, Huh7, and HepG2 cells were cultured in DMEM GlutaMAX, supplemented with 10% fetal calf serum and 1%

penicillin streptomycin solution. RAW 264.7 cells were cultured in RPMI medium GlutaMAX, supplemented with 10% fetal calf serum and 1% penicillin streptomycin. All cell lines were cultured at 5% CO<sub>2</sub> and 21% O<sub>2</sub>. HEK293T, Huh7, HepG2, and RAW264.7 cells, in which *COMMD1* and *COMMD6* were stably silenced using short hairpin RNA (detailed below), were selected by 1  $\mu$ g/mL puromycin. Primary hepatocytes were cultured as described previously.<sup>8</sup>

### RNA Interference

*COMMD1* was stably silenced in HEK293T and HepG2 cells using short hairpin RNA as previously described.<sup>17</sup> A plasmid encoding short hairpin RNA against *COMMD6* was generated by cloning a target sequence specific for human *COMMD6* (AATGACGATTCCACAGTTTCA) or mouse *COMMD6* (TGACAATTCCACAATTTCA) into the pLKO-TRC vector. HEK293T, HepG2, and RAW264.7 cell lines were infected with lentiviral particles carrying the pLKO-TRC or pLKO-shCOMMD6 vector.

### Sucrose Gradients

Male mice (wild type [WT] and *Commd1*<sup>ΔHep</sup>) were fasted for 4 hours and euthanized. Livers were isolated and processed as described previously.<sup>8</sup>

### Immunoprecipitation Analysis

Immunoprecipitation experiments were performed as described before.<sup>8</sup> In this study, HEK293T cells and primary hepatocytes were used. Mouse anti-COMMD1 (MAB7526; R&D Systems) antibodies were used to immunoprecipitate COMMD1; rabbit anti-COMMD6 (custom made<sup>25</sup>) was used to immunoprecipitate COMMD6. Normal IgG was used as a negative immunoprecipitation control.

### Gene Expression Analysis

Cells were grown to 70% confluency and lysed with QIAzol Lysis Reagent (Qiagen). Pieces of murine liver of  $\approx$ 100 mg were homogenized in 1 mL QIAzol Lysis Reagent (Qiagen). Total RNA was isolated by chloroform extraction. Isopropanol-precipitated and ethanol-washed RNA pellets were dissolved in RNase/DNase-free water. One microgram of RNA was used to prepare cDNA with the Transcriptor Universal cDNA Master kit (Roche), according to the manufacturer's protocol. Twenty nanograms of cDNA was used for subsequent quantitative real-time polymerase chain reaction using the FastStart SYBR Green Master (Roche) and 7900HT Fast Real-Time PCR System (Applied Biosystems).

### Western Blot

For Western blot, total cell lysates and liver homogenates were obtained using NP-40 buffer (0.1% nonidet P-40 [NP-40], 0.4 mol/L NaCl, 10 mmol/L Tris-HCl [pH 8.0], and 1 mmol/L EDTA) supplemented with protease and phosphatase inhibitors (Roche). Protein concentration was determined using the Bradford assay (Bio-Rad). Thirty micrograms of protein was separated using SDS-PAGE and transferred to Amersham Hybond-P PVDF Transfer Membrane (GE Healthcare; RPN303F). Membranes were blocked in 5% milk in tris-buffered saline with 0.01% Tween-20 and incubated with the indicated antibodies. Proteins were visualized using a ChemiDoc XRS+System (Bio-Rad) using Image Lab software version 5.2.1 (Bio-Rad).

### Antibodies

Antibodies used for Western blot and immunofluorescence are described in the [Online Data Supplement](#).

### Targeted Proteomics

To quantify the protein concentrations of the COMMDs, components of retromer, the CCC and WASH complexes, LDLR, LRP1, Apo (apolipoprotein) A1, ApoB100, and ApoB48 in the samples of the different mouse models, we developed targeted proteomics assay. Detailed description is provided in the [Online Data Supplement](#).

### Statistical Analysis

In vitro data were obtained from 3 independent experiments  $\pm$  SEM. Mouse data show average values  $\pm$  SEM, n=7 to 12. Analyses were

performed using GraphPad version 6.05 (GraphPad software). The Student *t* test was used to test for statistical significance between 2 groups. For all experiments, a *P* value of <0.05 was considered statistically significant.

## Results

### Hepatic *Commd6* Ablation Results in Increased Plasma LDL Cholesterol Levels

To understand the biological role of COMMD proteins in lipoprotein metabolism, we used COMMD6 as a prototype for the COMMD family, as COMMD6 primarily consists of the COMM domain,<sup>15</sup> a region of the COMMD proteins that is crucial for multiple protein–protein interactions, including the interaction with LDLR and the CCC core component CCDC22.<sup>8,9</sup> A *Commd6* conditional knockout mouse model was generated by flanking exon 3 of *Commd6* with *loxP* sites (Online Figure IA). Mouse genotypes were confirmed by Southern blot and polymerase chain reaction (Online Figure IB and IC). To assess the role of hepatic COMMD6 in lipoprotein metabolism, we deleted *Commd6* in hepatocytes by crossbreeding *Commd6<sup>F/F</sup>* mice with transgenic mice expressing Cre-recombinase specifically in hepatocytes (Alb-Cre).

Liver-specific *Commd6* knockout mice (*Commd6<sup>ΔHep</sup>*) were born in the expected Mendelian frequency, and the absence of COMMD6 in hepatocytes was validated on mRNA, and protein levels by quantitative real-time polymerase chain reaction and Western blot (Online Figure ID and IE). No overt differences were observed between hepatic *Commd6* knockout animals and *Commd6<sup>F/F</sup>* littermate controls (hereafter referred to as WT), with regard to body weight, liver weight, and liver histology (Online Figure IIA through IIC). However, hepatic COMMD6 deficiency resulted in a  $\approx 37\%$  increase ( $P < 0.01$ ) in plasma TC levels on a chow diet and a  $\approx 40\%$  increase ( $P < 0.001$ ) in plasma TC levels on a high-fat high-cholesterol (HFC) diet compared with WT animals (Figure 1A and 1B). Plasma triglyceride, hepatic cholesterol, and triglyceride concentrations were unaltered by hepatic *Commd6* ablation (Figure 1A and 1B). Using a specifically developed targeted proteomics approach, we observed that the plasma levels of ApoB100 were significantly elevated ( $P < 0.01$ ) in *Commd6<sup>ΔHep</sup>* mice, both on chow and HFC diet feeding (Figure 1C and 1D, insets). Plasma ApoA1 levels were also increased ( $P < 0.01$ ) in *Commd6<sup>ΔHep</sup>* mice but only after feeding chow diet and not on HFC diet feeding (Figure 1C and

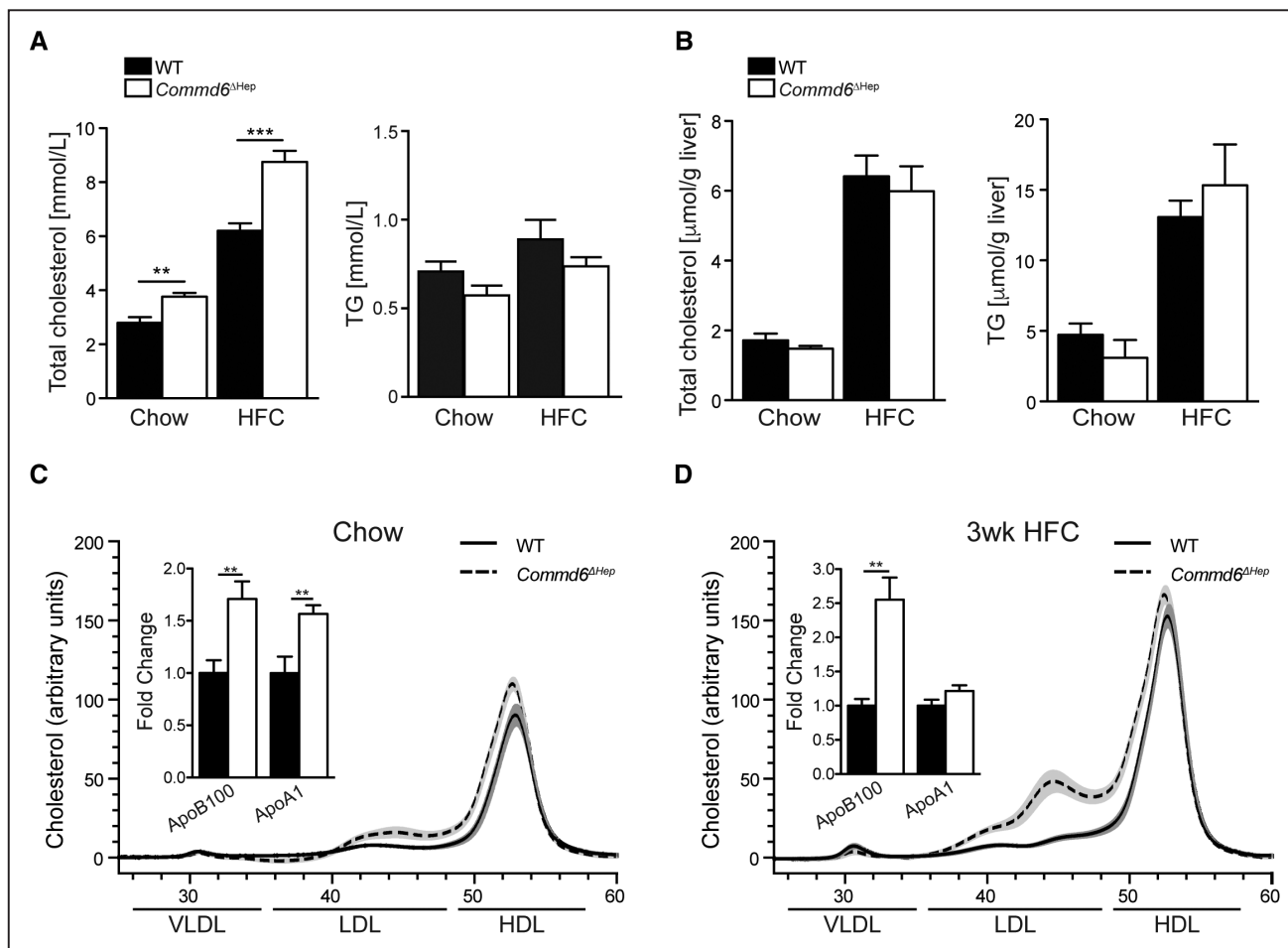


**Figure 1. Hepatic COMMD6 (copper metabolism MURR1 domain 6) deficiency increases plasma cholesterol levels.** Total cholesterol and triglyceride levels in plasma (A) and liver (B) of wild-type (WT) and *Commd6<sup>ΔHep</sup>* mice fed a chow or a high-fat high-cholesterol (HFC) diet for 1 wk ( $n=7-9$ ). The average total cholesterol levels of fast-performance liquid chromatography fractionated plasma of the experimental groups of mice fed either a chow (C) or a HFC (D) diet. Insets in C and D, Plasma Apo (apolipoprotein) B100 and ApoA1 levels of *Commd6<sup>ΔHep</sup>* and WT, indicated by fold change vs WT controls. Group averages and SEM are shown. \*\* $P < 0.01$ , \*\*\* $P < 0.001$  (compared with control groups).

1D, insets). In line with the elevated plasma ApoB100 levels, the lipoprotein profile of WT and *Commd6* $\Delta^{Hep}$  animals fed a chow or HFC diet (Figure 1C and 1D; Online Figure IID and IIE) showed an increase in plasma LDL cholesterol in *Commd6* knockout animals. Intriguingly, these data demonstrate that, similar to *Commd1*<sup>8</sup>, hepatic *Commd6* ablation causes hypercholesterolemia.

### COMMD6 Colocalizes With the WASH Complex and Retromer

Previous in vitro data indicated that COMMD1 and the WASH complex act together to facilitate endosomal trafficking of LDLR.<sup>9</sup> We investigated whether COMMD6 is also associated with the WASH complex on the endosome. Because there are no appropriate antibodies to determine the subcellular localization of COMMD6 by immunofluorescence staining, we used the CRISPR/Cas9 gene editing technology to fuse a V5-epitope tag to endogenous *COMMD6* in HEK293T cells. These cells were targeted with a sgRNA recognizing the stop codon of *COMMD6* and a corresponding repair template to incorporate the V5-tag before the stop codon (Online Figure IIIA). Immunofluorescence staining showed that COMMD6 strongly colocalizes with WASH1, FAM21, and COMMD1, almost to a similar degree as seen between COMMD1 and WASH1 and FAM21 (Online Figures IVA through IVC and VA). The recruitment of the WASH complex and COMMD1 to the endosomes rely on the retromer subunit VPS35,<sup>8,9,12</sup> and therefore, we examined COMMD6 localization relative to VPS35. COMMD6 overlapped with VPS35 almost to the same extent as COMMD1 and VPS35 (Online Figures IVA through IVC and VA). Next, we determined the effect of COMMD6 deficiency on the total and surface levels of LDLR in primary hepatocytes. Ablation of COMMD6 impaired the total expression and the expression of LDLR at the plasma membrane (Online Figure VB). Similar effect on the total and plasma membrane expression of LRP1 was seen (Online Figure VB). The reduced total LDLR and LRP1 levels can likely be explained by increased lysosomal degradation because of impaired receptor recycling, similar as seen in WASH1-deficient mouse fibroblast cells.<sup>8,26</sup> These observations indicate that both COMMD6 and COMMD1 are localized in a WASH and retromer-enriched subcompartment of the endosome and suggest that COMMD6 may also participate in the CCC–WASH axis in endosomal sorting of receptors, including LDLR and LRP1.

### COMMD6 Is Indispensable for COMMD1, CCDC22, and CCDC93 Protein Expression

To further evaluate the biological role of COMMD6 in CCC complex functioning, we stably downregulated *COMMD6* expression in cells of different origins. The protein and mRNA levels of COMMD6 were both markedly reduced in HEK293T and RAW264.7 cells expressing short hairpin RNA targeting *COMMD6* (Figure 2A and 2B). Unexpectedly, silencing of *COMMD6* significantly decreased COMMD1 protein levels (Figure 2A) without affecting *COMMD1* mRNA (Figure 2B). However, silencing of *COMMD1* did not reduce COMMD6 protein levels (Figure 2A). Taken the effect of liver-specific ablation of *Commd6* on plasma lipid levels, we also silenced *COMMD6* in the hepatocellular carcinoma cell

lines HepG2 and Huh7 and found similar effects as described above (Figure 2C). To assess whether reduced COMMD1 levels in COMMD6 knockdown cells are caused by increased proteasomal degradation of COMMD1, we treated control and COMMD6 knockdown cells (HEK293T and RAW264.7) with the proteasomal inhibitor MG132. Blocking proteasome activity partially restored COMMD1 protein levels in COMMD6 knockdown cell lines (Figure 2D), suggesting that COMMD1 instability is partially ubiquitin dependent. In line with previous studies,<sup>15,25</sup> we observed that COMMD1 and COMMD6 are physically associated with each other, as determined by coimmunoprecipitation assay (Figure 2E).

The results of COMMD6 ablation on COMMD1 levels in different cell lines led us to investigate the effect of hepatic COMMD6 inactivation on the protein levels of COMMD1 and the CCC components CCDC22 and CCDC93 in mice. As observed in COMMD6 knockdown cells, depletion of *Commd6* in mouse hepatocytes blunted COMMD1 protein levels, accompanied by reduced protein levels of the CCC core components CCDC22 and CCDC93 (Figure 2F). The decreased COMMD1, CCDC22, and CCDC93 levels were not caused by aberrant gene expression (Figure 2G). These data indicate that COMMD6 form a protein complex with COMMD1 that is indispensable for the protein stability of CCC complex in endosomal receptor recycling.

### Stability of COMMD Proteins Associated With the CCC Complex Depends on Other COMMD Proteins

Because all COMMDs can participate in the CCC complex through an interaction with CCDC22,<sup>16</sup> this prompted us to assess whether COMMD6 deficiency also affects the protein levels of other COMMD family members. Deletion of hepatic *Commd6* markedly decreased all detectable COMMD proteins (Figure 3A), however, not all to the same degree (Figure 3A), as COMMD3 levels were only moderately decreased compared with other COMMD proteins (Figure 3A). The adverse effect of *Commd6* deletion on COMMD1 protein levels made us to decide to also assess the consequence of hepatic COMMD1 deficiency on the protein levels of COMMDs in mice. The effect of hepatic *Commd1* deletion on COMMD protein amounts was similar to *Commd6* depletion (Figure 3A and 3B).

Given the difficulty in detecting all COMMD proteins using specific antibodies, we measured the COMMD protein concentrations in liver homogenates with specifically developed targeted proteomics assays. We used isotopically labeled standards combined with liquid chromatography-mass spectrometry analysis for accurate quantification of the proteins studied.<sup>27</sup> In line with the Western blot results, hepatic *Commd1* and *Commd6* depletion in mice significantly reduced the expression of all COMMD proteins (Figure 3C; Online Table I). Furthermore, the CCC core subunits were reduced by  $\approx 70\%$  ( $P < 0.05$ ) in COMMD1- and COMMD6-deficient livers (Figure 3C; Online Table I), whereas the expression of the retromer subunits, LDLR and LRP1, were unaffected (Figure 3C; Online Table I). Intriguingly, the expression of the WASH component WASH1 was increased by  $\approx 50\%$  ( $P < 0.05$ ) after loss of COMMD1 or COMMD6. Altogether,

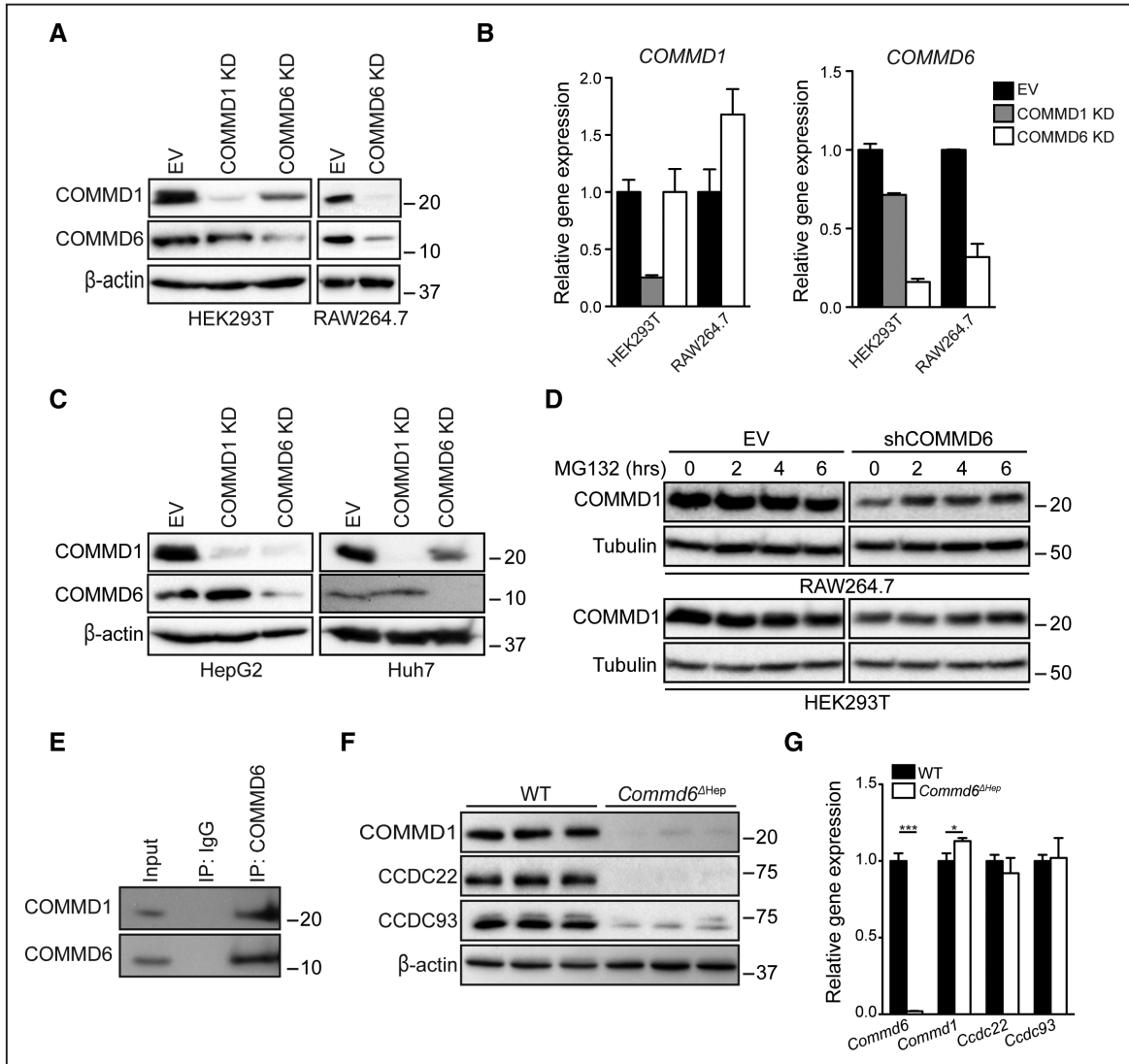


**Figure 2. COMMD6 (copper metabolism MURR1 domain 6) inactivation downregulates COMMD1 in different cell lines.** **A**, COMMD1 and COMMD6 protein levels in HEK293T and RAW264.7 cell lines with stable silencing of COMMD1 (COMMD1 knockdown [KD]) or COMMD6 (COMMD6 KD) and control cells (empty vector [EV]) determined by immunoblotting. **B**, Relative mRNA levels of *COMMD1* and *COMMD6* in COMMD1 KD and COMMD6 KD HEK293T and RAW264.7 cell lines. Average values and SEM are shown ( $n=3$ ). **C**, COMMD1 and COMMD6 protein levels in hepatocellular carcinoma cell lines HepG2 and Huh7 with stable silencing of COMMD1 (COMMD1 KD) or COMMD6 (COMMD6 KD) and control cells (EV) determined by immunoblotting. **D**, Western blotting for COMMD1 and tubulin in control and COMMD6 KD HEK293T and RAW264.7 cells treated with proteasome inhibitor MG132 for 0, 2, 4, and 6 h. **E**, Endogenous COMMD6 immunoprecipitations in HEK293T cells. Immunoprecipitates were washed, separated by SDS gel electrophoresis, and immunoblotted as indicated. **F**, Protein levels of COMMD1, CCDC22, and CCDC93 in livers of WT and *Commd6* $\Delta$ Hep determined by immunoblot analysis. **G**, *Commd1*, *Ccdc22*, and *Ccdc93* expression in livers of *Commd6* $\Delta$ Hep and WT mice ( $n=7-9$ ). Group averages with SEM are shown.

these results suggest that the integrity of CCC core complex (CCDC22, CCDC93, and C16orf62) and the protein expression of all COMMDs depend on the expression of COMMD1 and COMMD6.

Although the amount of most COMMD proteins was reduced by  $\approx 70\%$  in *Commd1* and *Commd6* knockout livers compared with WT livers ( $P<0.05$ ), COMMD3 protein levels were only decreased by  $\approx 50\%$  ( $P<0.05$ ). To understand which fraction of COMMD3 is adversely affected by COMMD1 deficiency, we assessed the relative distribution of COMMD1 and COMMD3 within CCC-, WASH- and retromer-positive endocytic compartments in cells using sucrose gradient fractionation. In WT livers, COMMD1 and COMMD3 had a

similar distribution and partially cosedimented with vesicles containing the CCC (CCDC22 and CCDC93) and WASH (WASH1 and FAM21) complexes. Furthermore, a percentage of COMMD1 and COMMD3 were present in the same fractions as LDLR (Figure 4A). Hepatic COMMD1 inactivation not only blunted the expression of CCDC22 and CCDC93 (Figure 4A) but also markedly abolished COMMD3 associated with the CCC and WASH complexes and LDLR, without affecting COMMD3 present in other fractions (Figure 4A). These results suggest that the main disturbance of COMMD3 levels on COMMD1 deficiency is on the fraction of COMMD3 that is associated with the CCC and WASH complexes and LDLR.

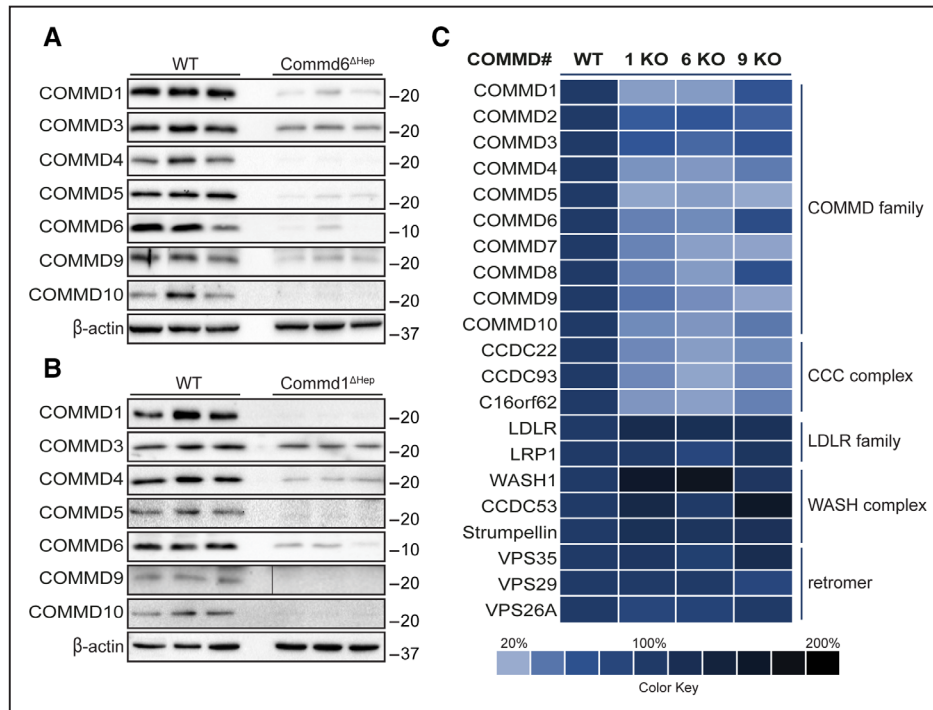


**Figure 3. Hepatic *Commd* deletion perturbs the protein stability of the complete COMMD (copper metabolism MURR1 domain) family.** Immunoblotting to determine COMMD protein levels in livers of wild-type (WT), *Commd6*<sup>ΔHep</sup> (A), and *Commd1*<sup>ΔHep</sup> (B) mice. C, Hepatic expression of COMMD protein, CCC (COMMD–CCDC22–CCDC93) complex, LDLR (low-density lipoprotein receptor) family, WASH (Wiskott–Aldrich syndrome protein and SCAR homologue) complex, and retromer determined by QconCAT technology. Color code depicts relative protein expression in livers of *Commd1*<sup>ΔHep</sup>, *Commd6*<sup>ΔHep</sup>, and *Commd9*<sup>ΔHep</sup> mice compared with WT mice (n=4).

To assess whether all COMMD proteins and CCC core subunits bind to COMMD1 in mouse primary hepatocytes, we measured the amount of COMMD and CCC core molecules in COMMD1 immunoprecipitates using a targeted proteomics approach. We found that all COMMD and CCC core proteins interact with COMMD1 (Figure 4B). These proteins were not detected in IgG negative control immunoprecipitates.

The association of COMMD1 with all COMMD proteins made us decide to investigate the role of other COMMDs on the protein stability of the COMMD family and CCC core subunits. We quantified the COMMD and CCC proteome also in *Commd9*<sup>ΔHep</sup> livers by proteomics analysis. Ablation of *Commd9* reduced the expression of the CCC complex subunits CCDC22, CCDC93, and C16orf62 ( $P<0.05$ ) to a similar extent as COMMD1 or COMMD6 inactivation (Figure 3C; Online Table I). However, COMMD9 seems to be less essential for COMMD stability, because COMMD1, 2, 3, 6, and 8 expression were only reduced by 40% to 50% ( $P<0.05$ ) after *Commd9* depletion (Figure 3C). This partial reduction in COMMD1 and COMMD6 levels was confirmed by Western blot analysis (Figure 4C and 4D).

Heterozygous loss of *Commd1* or *Commd6* does not alter plasma cholesterol levels (B. van de Sluis, unpublished data, 2017),<sup>8,10</sup> and because COMMD1 and COMMD6 levels were only reduced by  $\approx 40\%$  in COMMD9-deficient livers (Figure 3C; Online Table I), this led us to investigate the effect of hepatic COMMD9 deficiency on plasma TC levels. Ablation of hepatic *Commd9* increased plasma TC levels ( $P<0.001$ ) and ApoB100 levels ( $P<0.001$ ), including plasma LDL cholesterol (Online Figure VIA and VIB), to a similar degree as

hepatic *Commd1*<sup>5</sup> or *Commd6* depletion (Figure 1A), without affecting body weight, liver weight, or liver histology (Online Figure VIC and VID).

Taken together, these results indicate that the protein expression of COMMDs relies on each other through forming multiprotein complexes, and the degree of dependency differs between COMMD proteins. In contrast, the stability of the CCC core components (CCDC22, CCDC93, and C16orf62) seems to be entirely dependent on the COMMD proteins. This specific decrease in the CCC core components in all 3 models of hepatic COMMD deficiency coincides with elevated plasma cholesterol levels.

### Hepatic Ablation of the CCC Component CCDC22 Increases Circulating Cholesterol Levels

To directly examine whether this specific loss of the CCC core underlies the increased circulating plasma cholesterol in our mouse models, we targeted one of its key component *Ccdc22* in hepatocytes of mouse livers using CRISPR/Cas9 gene editing technology. Three gRNAs were designed to simultaneously target exon 1 and exon 2 of *Ccdc22* (Online Figure VIIA). These gRNAs (Ad-gRNA\_Ccdc22) were directed to the liver of either WT or liver-specific Cas9-expressing C57BL/6J mice using an adenoviral gene delivery system. One week before virus administration, blood was collected to ensure the plasma cholesterol values of WT and Cas9-expressing C57BL/6J mice were similar (Online Figure VIIIB). Twenty-one days after virus injection, blood and tissues were collected for analysis (Online Figure VIIIB). Hepatic expression of the 3 gRNAs reduced CCDC22 expression by  $\approx 70\%$  and

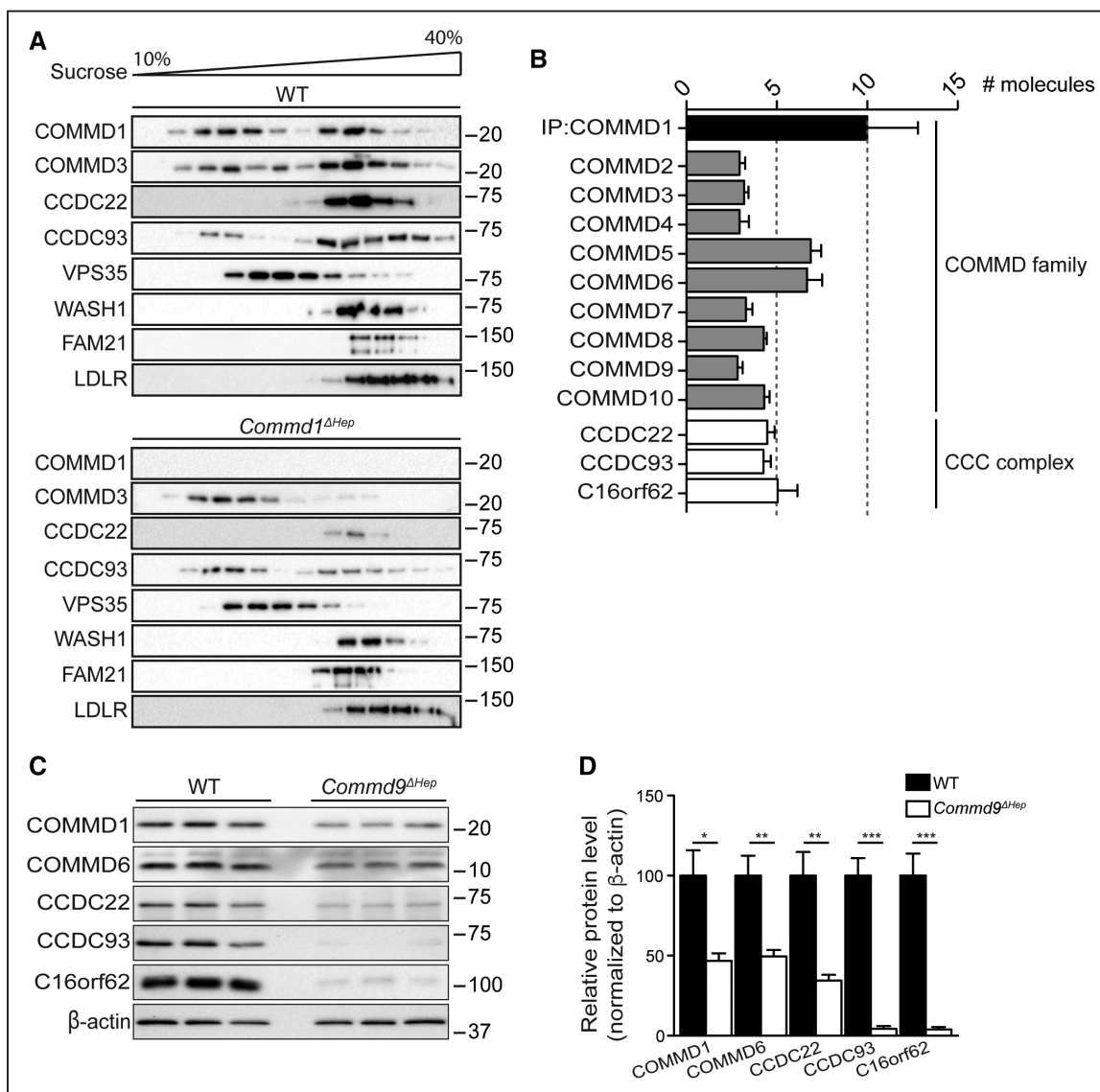


**Figure 4.** Depletion of either COMMD1 (copper metabolism MURR1 domain 1) or COMMD9 perturbs the formation of the CCC (COMMD–CCDC22–CCDC93) complex. **A**, Western blotting of wild-type (WT) and *Commd1* knockout (KO) mouse liver homogenates fractionated by ultracentrifugation on 10% to 40% sucrose gradient. **B**, Number of COMMD and CCC core components associated with COMMD1 in primary hepatocytes as determined by immunoprecipitation assay and subsequently targeted proteomics analysis (n=5). **C**, COMMD1, COMMD6, CCDC22, and CCDC93 protein expression in livers of WT and *Commd9*<sup>ΔHep</sup> were determined by immunoblotting. **D**, Quantification of Western blot results depicted in **C**. Group averages and SEM are shown. \**P*<0.05, \*\**P*<0.01, \*\*\**P*<0.001 (compared with control groups).

diminished the levels of CCDC93, C16orf62, and COMMD1 (Figure 5A and 5B). Targeted proteomics analysis showed that the expression of all COMMD proteins was significantly reduced by targeting *Ccdc22*, with the exception of COMMD6 (Online Figure VIIC). CCDC22 inactivation did not alter the body weight, liver weight, or cause overt liver pathology (Online Figure VIIC and VIID), but it increased plasma TC levels by ≈35% (*P*<0.01) compared with WT mice injected with Ad-gRNA-*Ccdc22* (Figure 5C). Lipoprotein fractionation by fast-performance liquid chromatography revealed that increased plasma cholesterol levels were because of increased plasma LDL cholesterol (Figure 5D), supported by the increased plasma ApoB100 levels (Figure 5E). In summary, these results indicate that proper formation of the core of

the CCC complex in hepatocytes is required to control plasma LDL cholesterol levels.

### Hepatic CCC Complex Ablation Exacerbates Hyperlipidemia and Accelerates Atherosclerosis

The reduced surface levels of both LDLR and LRP1 on inactivation of the CCC complex (Online Figure VB) suggest that the CCC complex orchestrate the trafficking of both receptors. Because LDLR can compensate for the loss of LRP1, studying LRP1 functioning in the clearance of plasma ApoE- and ApoB-containing particles in mice is only possible in a hepatic LDLR-deficient background.<sup>28</sup> To assess the role of CCC complex in LRP1 functioning, we overexpressed a gain-of-function variant of PCSK9 (proprotein convertase subtilisin/kexin type 9)-D377Y in the liver of WT and



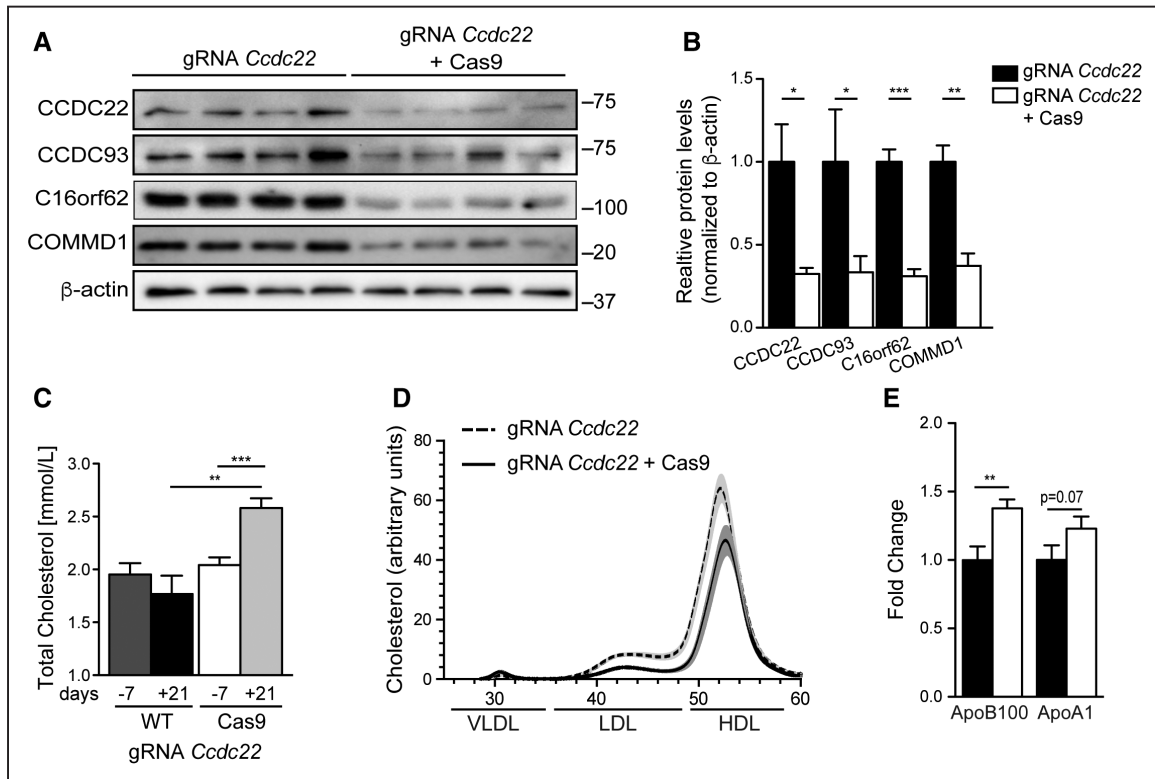


**Figure 5. Hepatic CRISPR/Cas9-mediated *Ccdc22* editing increases plasma cholesterol levels.** **A**, Protein levels of CCDC22, CCDC93, and COMMD1 determined by immunoblotting. **B**, Quantification of immunoblot results depicted in **A**. **C**, Total cholesterol levels in of wild-type (WT) and Cas9 mice on chow, 7 d before and 21 d after injection with Ad-gRNA-Ccdc22 (n=5–6). **D**, The average total cholesterol levels of fast-performance liquid chromatography fractionated plasma of WT and Cas9 mice 21 d after Ad-gRNA-Ccdc22 injection. **E**, Plasma Apo (apolipoprotein) B100 and ApoA1 levels of WT and hepatic CCDC22 deficient mice, indicated by fold change vs WT controls (n=4–6). Group averages and SEM are shown. \* $P < 0.05$ , \*\* $P < 0.01$ , \*\*\* $P < 0.001$  (compared with control groups).

*Commd1* $\Delta^{\text{Hep}}$  mice by injecting an adeno-associated virus-expressing human PCSK9-D377Y<sup>29</sup> into the mouse veins. PCSK9-D377Y expression blunted the protein expression of LDLR, but not LRP1, in the liver of WT and *Commd1* $\Delta^{\text{Hep}}$  mice (Figure 6A). As expected, LDLR deficiency led to a significant increase in plasma TC and triglyceride (Figure 6B) in WT mice. Animals that lack the protein expression of both COMMD1 and LDLR showed higher increase in plasma TC and triglyceride levels compared with mice only deficient for LDLR in the liver (Figure 6B). The plasma concentrations of ApoB100 and ApoB48 were examined by Coomassie staining and showed that LDLR deficiency resulted in a marked increase in both apolipoproteins (Figure 6C). In contrast, hepatic ablation of both LDLR and COMMD1 further increased ApoB48 levels compared with control animals (Figure 6C). This dramatic increase in ApoB48 in mice deficient for both COMMD1 and LDLR is supported by targeted proteomics analysis of the plasma samples of both groups in which we specifically determined the plasma concentration of ApoB100 and ApoB48 (Figure 6D). This further rise in both plasma TC and ApoB48 levels was also reflected by the marked change in their plasma lipoprotein profile (Figure 6E). Hepatic deficiency of both COMMD1 and LDLR led to a large increase of plasma lipoproteins in the chylomicron remnant/very-low-density lipoprotein and LDL size range. A similar increase in plasma ApoB48 levels and change in lipoprotein profile has been seen on hepatic

depletion of both *Ldlr* and *Lrp1*,<sup>28</sup> suggesting that the CCC complex also facilitates the functioning of LRP1.

Next, we investigated the contribution of CCC-mediated endosomal LDLR/LRP1 trafficking on the progression of atherosclerosis. We used ApoE3\*Leiden (ApoE3\*L) transgenic mice as a model for atherosclerosis<sup>30</sup> because these mice are hyperlipidemic, develop atherosclerosis, and express LDLR in their livers,<sup>31</sup> which we thought to be essential in evaluating the contribution of the CCC complex to dyslipidemia and atherogenesis. Liver-specific *Commd1* knockout (*Commd1* $\Delta^{\text{Hep}}$ ) mice were crossbred with ApoE3\*L mice to ablate *Commd1* in hepatocytes (ApoE3\*L;*Commd1* $\Delta^{\text{Hep}}$ ). Hepatic COMMD1 deficiency did not affect the total protein expression of LDLR and LRP1 in the liver of ApoE3\*L (Online Figure VIIIA) mice fed a HFC diet for 12 weeks but resulted in a dramatic rise in plasma TC and triglyceride levels ( $\approx 100\%$  increase;  $P < 0.001$ ; Figure 7A). Very-low-density lipoprotein cholesterol and LDL cholesterol levels were notably increased by inactivation of the CCC complex (Figure 7B), supported by the increased plasma ApoB100 levels. This rise in plasma cholesterol levels coincided with  $\approx 50\%$  larger atherosclerotic lesion area ( $P < 0.01$ ) in the aortic root of these animals (Figure 7C and 7D). Atherosclerotic lesions in the aortic root were small and foam-cell rich (Figure 7C and 7D). We then assessed atherosclerotic lesion area in the aortic arch by performing en face analysis using Oil Red O staining. We observed no atherosclerotic lesions

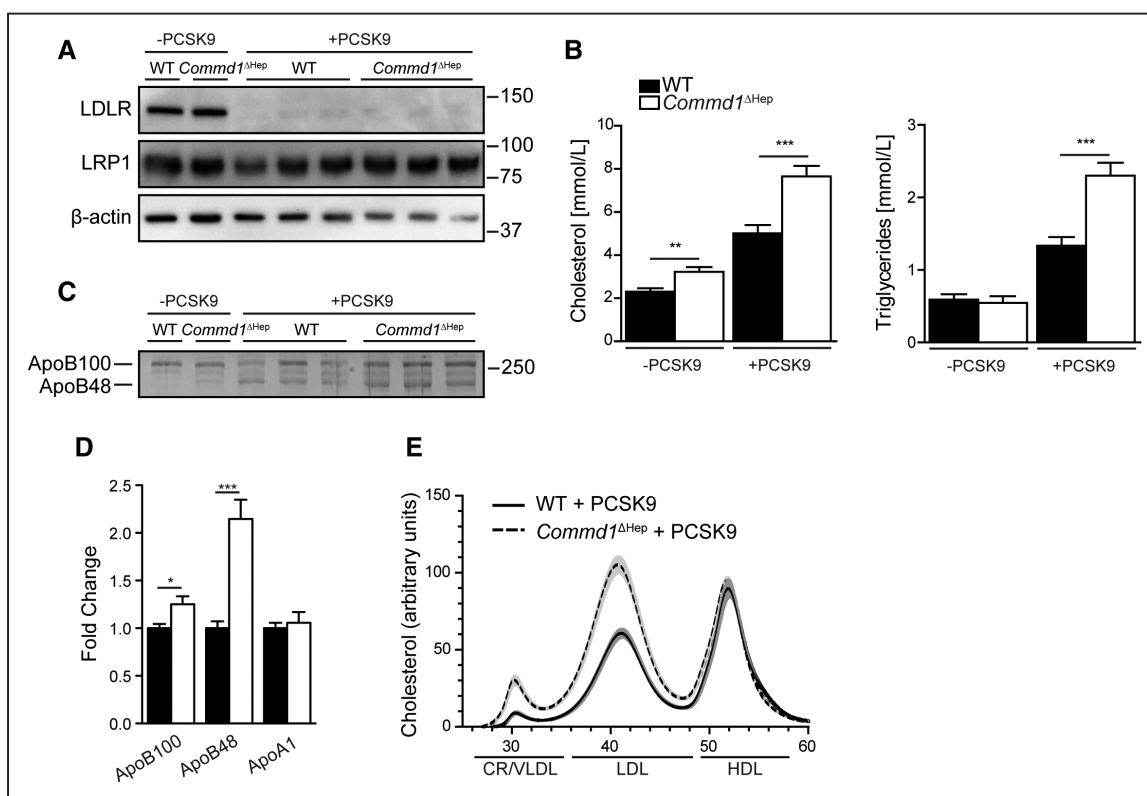


**Figure 6. CCC (COMMD–CCDC22–CCDC93) complex inactivation further increases dyslipidemia in hepatic LDLR (low-density lipoprotein receptor)-deficient mice.** **A**, Hepatic LDLR and LRP1 (LDLR-related protein 1) levels of uninjected and adeno-associated virus (AAV)-PCSK9 (proprotein convertase subtilisin/kexin type 9)-D377Y-injected wild-type (WT) and *Commd1*<sup>ΔHep</sup> mice. **B**, Plasma total cholesterol and triglyceride levels of WT and *Commd1*<sup>ΔHep</sup> mice before and 3 wk after injection of AAV-PCSK9-D377Y (n=9–10). **C**, Plasma of uninjected and AAV-PCSK9-D377Y-injected WT and *Commd1*<sup>ΔHep</sup> mice was separated by SDS gel electrophoresis and ApoB100 and ApoB48 was visualized by Coomassie staining. **D**, Plasma ApoB100, ApoB48, and ApoA1 levels of WT and *Commd1*<sup>ΔHep</sup> mice 3 wk after injection of AAV-PCSK9-D377Y (n=6). **E**, Average total cholesterol in fast-performance liquid chromatography fractionated plasma of AAV-PCSK9-D377Y-injected WT and *Commd1*<sup>ΔHep</sup> mice (n=9–10). Group averages and SEM are shown. \**P*<0.05, \*\**P*<0.01, \*\*\**P*<0.001 (compared with controls).

in the aortic arch of both genotypes (Online Figure VIII B), indicating that atherosclerosis did not yet develop in this part of the aorta. Taken together, hepatic perturbations in the CCC complex exacerbates hyperlipidemia—likely because of a defect in LDLR and LRP1-mediated lipoprotein clearance—and accelerates atherosclerosis in ApoE3\*L mice.

## Discussion

Removal of atherogenic LDL cholesterol from the circulation is highly dependent on hepatic LDLR, and progress has been made in our understanding of how LDL trafficking is mechanistically coordinated. Recently, the CCC complex—a multiprotein complex associated with vital elements of the endocytic sorting machinery<sup>9</sup>—was identified as a novel factor of endosomal LDLR trafficking (Online Figure IX).<sup>8</sup> In this study, we revealed that the integrity of the CCC core components, namely, CCDC22, CCDC93 and C16orf62, is not exclusively controlled by COMMD1,<sup>8</sup> but by numerous members of the COMMD family (Online Figure IX). In addition, our data also suggest that the stability of the COMMDs in hepatocytes relies on the CCC core component CCDC22, indicating a strong interrelation between the COMMD family and the core of the CCC complex in endosomal trafficking of cell surface receptors, including LDLR and LRP1.<sup>8</sup>

It has been implicated that the COMMDs form heterogeneous CCC complexes that facilitate receptor-specific endosomal trafficking,<sup>9,18,21,22</sup> but their contribution in the formation of the CCC complex in endosomal LDLR trafficking was still unclear. To investigate this, we generated and characterized different liver-specific *Commd* knockout mouse models (*Commd1*, *Commd6*, and *Commd9*), and we identified for the first time that the stability of the core of the CCC complex depends on numerous COMMDs, as CCDC22, CCDC93, and C16orf62 levels were massively reduced on hepatic deletion of *Commd1*, *Commd6*, or *Commd9*. This loss of the CCC core subunits was correlated with elevated plasma LDL cholesterol levels in all our models,<sup>8</sup> indicating that specific disruption of the CCC core leads to the hypercholesterolemic phenotype.<sup>8,11</sup> Indeed, using CRISPR/Cas9-mediated somatic gene targeting, we achieved extensive reduction in hepatocyte CCDC22 levels and provided evidence for a direct role for the core of the CCC complex in the regulating of plasma cholesterol levels in mice. In addition, we found that perturbation in the CCC complex contributes in the progression of atherosclerosis in ApoE3\*L mice, a mouse model with a human-like lipoprotein profile. Although the total protein levels of hepatic LDLR and LRP1 in WT and ApoE3\*L mice are not affected on CCC inactivation, this study and our previous work<sup>8</sup> showed

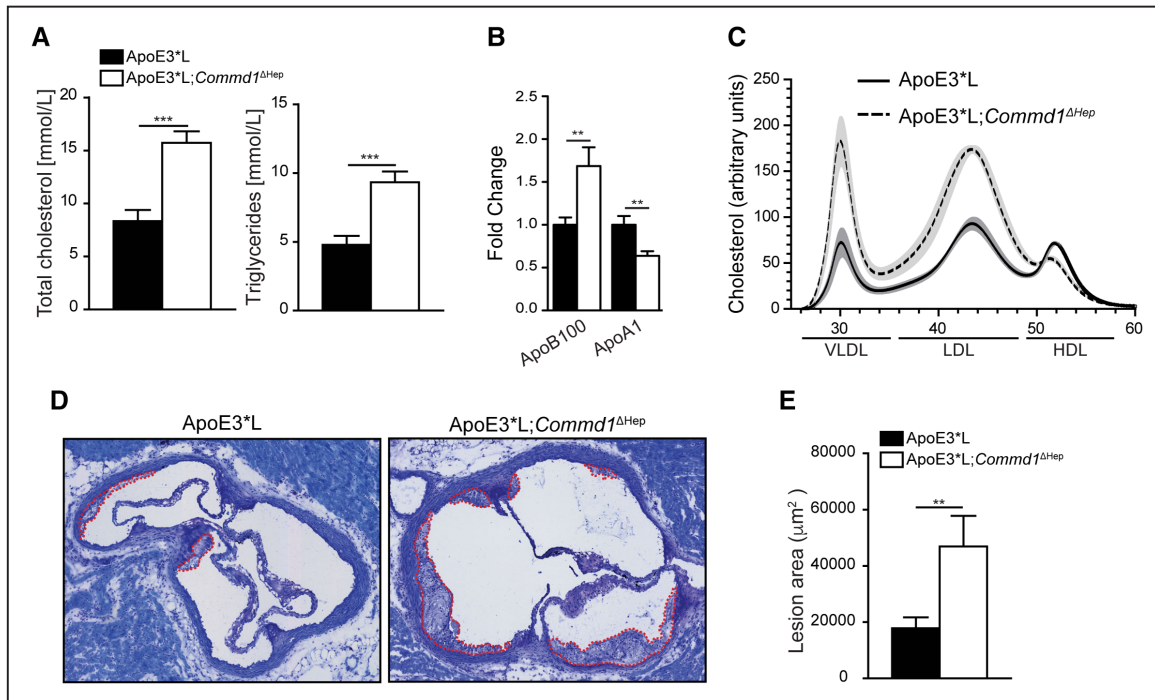


**Figure 7. Destabilization of the CCC (COMMD-CCDC22-CCDC93) complex exacerbates dyslipidemia and atherosclerosis.** **A**, Total cholesterol and triglyceride levels in plasma of ApoE3\**L* and ApoE3\**L*; *Commd1*<sup>ΔHep</sup> mice fed a high-fat high-cholesterol (HFC) diet for 12 wk (n=8–11). **B**, Average total cholesterol in fast-performance liquid chromatography fractionated plasma of mice fed a HFC diet for 12 wk. **C**, Representative images of toluidin blue staining of aortic root of ApoE3\**L* and ApoE3\**L*; *Commd1*<sup>ΔHep</sup> mice after 12 wk of HFC feeding. **D**, Quantification of plaque size in ApoE3\**L* and ApoE3\**L*; *Commd1*<sup>ΔHep</sup> mice after 12 wk of HFC feeding. **E**, Lesion area is the average of 10 cross-sections per animal (n=8–11). Group averages and SEM are shown. \*\**P*<0.01, \*\*\**P*<0.001 (compared with controls).

that hepatic CCC deficiency reduces surface levels of LDLR and LRP1—likely because of impaired endosomal receptor trafficking<sup>8</sup>—leading to increased plasma LDL cholesterol levels and accelerated atherosclerosis (Online Figure IX). In humans, mutations in *CCDC22* cause the severe developmental disorder X-linked intellectual disability, and we recently showed that the *CCDC22* mutations are also correlated with hypercholesterolemia in these patients.<sup>8</sup> Now, we provide genetic evidence that *CCDC22* insufficiency directly cause high plasma LDL cholesterol levels in X-linked intellectual disability patients and establish that CCC complex-mediated LDLR trafficking is conserved between mice and humans. However, whether human genetic variants in *COMMDs*, *CCDC93*, and *C16orf62* exist and those are associated with plasma lipid levels and cardiovascular events needs to be validated.

This study shows also for the first time that the expression of the COMMD proteins in hepatocytes relies on each other, but intriguingly, the degree of dependency differs between COMMD proteins. For example, COMMD5 and COMMD10 are reduced by ≈70%, whereas COMMD3 is only diminished by 50% on *Commd1*, *Commd6*, or *Commd9* depletion. The exact reason for these differences is unclear, but our cell fractionation experiments showed that only the fraction of COMMD3 proteins associated with the CCC and WASH complexes are adversely affected after *Commd1* deletion. These results suggest that the portion of the COMMDs assembled into the CCC complexes is particularly disturbed by removal of another COMMD protein. The fraction of a COMMD protein that is not affected by the loss of another COMMD protein is likely present in other cellular compartments, where

they likely mediate other biological activities of these factors, similarly to what has been reported for COMMD1, which can also regulate NF-κB (nuclear factor kappa B) and HIF-1 (hypoxia inducible factor 1) signaling.<sup>17,19,32</sup>

The reduction of all COMMDs and the CCC core subunits (CCDC22, CCD93, and C16orf62) on loss of any COMMD studied is remarkably, which mystifies the biological relevance of hepatic expression of 10 different COMMD proteins that are all assembled into a CCC complex.<sup>9,18,21,22</sup> Because only COMMD5 and COMMD9 regulate Notch receptor recycling<sup>18</sup> and only a few COMMDs, including COMMD1, bind to the copper transporting protein ATP7B to mediate its trafficking,<sup>11</sup> it has been postulated that the COMMDs define different CCC complexes that act in conjunction with the WASH complex for selective endosomal trafficking of transmembrane proteins. We now show that in addition to COMMD1, also COMMD3 and COMMD6 are associated with the WASH complex.<sup>9</sup> On the basis of these novel findings, it is reasonable to speculate that elevated plasma LDL cholesterol after downregulation of one COMMD protein is indirect and is the consequence of destabilizing of different CCC complexes, including the CCC complex that directly mediates endosomal LDLR sorting. Further studies are needed to elucidate the stoichiometry of these heterogeneous CCC complexes in receptor-specific endosomal trafficking.

We recently speculated that LDLR is retrieved by SNX17 (sorting nexin 17) from the lysosomes before LDLR is transferred to the CCC and WASH complexes for endosomal recycling (Online Figure IX).<sup>8</sup> SNX17 (sortin nexin 17) also facilitates endosomal trafficking of the LRP1.<sup>33–35</sup> LDLR and LRP1 contain a NPxY motif in their cytoplasmic tail,

and both SNX17 and COMMD1 can bind to this NPxY motif,<sup>8,35–37</sup> suggesting that the CCC complex can facilitate the endosomal trafficking of various members of the LDLR family that contain this motif, including LRP1.<sup>38</sup> Indeed, our in vitro and in vivo results indicate that the functioning of LDLR and LRP1 are both affected by inactivation of the CCC complex (Online Figure IXB). We, therefore, speculate that on entering the endosomes, LDLR and LRP1 are coupled to SNX17 and are recycled by CCC and WASH complexes.<sup>8</sup> McNally et al<sup>34</sup> recently identified a multiprotein complex, called retriever, which is composed of DSCR3, VPS29, and C16orf62. In this study, the authors suggest that C16orf62 does not belong to the CCC complex but participate in the retriever as a separate complex in the CCC–WASH axis.<sup>34</sup> This is an interesting observation, as our study implies that C16orf62 does participate in the CCC complex because ablation of either *Ccdc22* or a *Commd* gene leads to a dramatic reduction in C16orf62 levels. In contrast, a decrease in C16orf62 levels has not been seen in HeLa cells deficient for both CCDC22 and CCDC93.<sup>34</sup> The exact reason for these opposite results is unclear, but it might be that loss of the CCC complex results in mislocalization of C16orf62—as the recruitment of the retriever to the endosomes relies on the CCC and WASH complexes<sup>34</sup>—that may eventually lead to proteolysis of this protein in hepatocytes. Further research is, therefore, needed to fully understand the molecular organization of the SNX17–retriever–CCC–WASH axis in coordinating the endosomal recycling of receptors, including LDLR and LRP1 (Online Figure IX).

We speculate that PCSK9 prevents LDLR to be recognized by the CCC–WASH axis and directly targets LDLR for proteolysis, a process that is independent of ESCRT (endosomal sorting complexes required for transport machinery).<sup>39</sup> Receptors that are not retrieved and recycled by the CCC–WASH axis are sorted into the lysosome for proteolysis, a process likely mediated by ESCRT (Online Figure IXA).<sup>34</sup> Therefore, we hypothesize that the PCSK9-mediated LDLR degradation and CCC-dependent LDLR recycling pathways are acting independently of each other, but further research is needed to understand the relation between these 2 pathways.

Interestingly, our data show that hepatic ablation of *Commd1*<sup>8</sup> and *Commd6* in mice fed a chow diet also lead to elevated plasma high-density lipoprotein cholesterol levels. Plasma high-density lipoprotein cholesteryl esters uptake is mediated by the SR-B1 (scavenger receptor class B member 1). Because different studies have shown that SR-B1 can be endocytosed,<sup>40</sup> this may indicate that the CCC complex has also a role in SR-B1–mediated high-density lipoprotein cholesteryl esters uptake, but further studies are warranted.

Collectively, our study has uncovered a previously unknown role for the evolutionarily conserved COMMD proteins in maintaining the integrity and function of the hepatocyte CCC complex during endosomal LDLR and LRP1 trafficking.

## Acknowledgments

We would like to dedicate this article to Marten Hofker, who passed away during the finalization of the article.

## Sources of Funding

This research was financially supported by the Netherlands Organization for Scientific Research (NWO-ALW grant 817.02.022 to B. van de Sluis), TransCard FP7-603091–2, the Jan Kornelis de Cock Stichting, the Graduate School for Drug Exploration (GUIDE), and the University of Groningen.

## Disclosures

None.

## References

1. Brown MS, Goldstein JL. A receptor-mediated pathway for cholesterol homeostasis. *Science*. 1986;232:34–47.
2. Goldstein JL, Hobbs HH, Brown MS. Familial hypercholesterolemia. In: Scriver CR, Beaudet AL, Valle D, eds. *The Metabolic and Molecular Bases of Inherited Disease*. 8th ed. New York, NY: McGraw-Hill, Inc; 2001:2863–2913.
3. van de Sluis B, Wijers M, Herz J. News on the molecular regulation and function of hepatic low-density lipoprotein receptor and LDLR-related protein 1. *Curr Opin Lipidol*. 2017;28:241–247.
4. Wijers M, Kuivenhoven JA, van de Sluis B. The life cycle of the low-density lipoprotein receptor: insights from cellular and in-vivo studies. *Curr Opin Lipidol*. 2015;26:82–87. doi: 10.1097/MOL.000000000000157.
5. Benjannet S, Rhainds D, Essalmani R, et al. NARC-1/PCSK9 and its natural mutants: zymogen cleavage and effects on the low density lipoprotein (LDL) receptor and LDL cholesterol. *J Biol Chem*. 2004;279:48865–48875. doi: 10.1074/jbc.M409699200.
6. Zelcer N, Hong C, Boyadjian R, Tontonoz P. LXR regulates cholesterol uptake through Idol-dependent ubiquitination of the LDL receptor. *Science*. 2009;325:100–104. doi: 10.1126/science.1168974.
7. Lagace TA, Curtis DE, Garuti R, McNutt MC, Park SW, Prather HB, Anderson NN, Ho YK, Hammer RE, Horton JD. Secreted PCSK9 decreases the number of LDL receptors in hepatocytes and in livers of parabiotic mice. *J Clin Invest*. 2006;116:2995–3005. doi: 10.1172/JCI29383.
8. Bartuzi P, Billadeau DD, Favier R, et al. CCC- and WASH-mediated endosomal sorting of LDLR is required for normal clearance of circulating LDL. *Nat Commun*. 2016;7:10961. doi: 10.1038/ncomms10961.
9. Phillips-Krawczak CA, Singla A, Starokadomskyy P, et al. COMMD1 is linked to the WASH complex and regulates endosomal trafficking of the copper transporter ATP7A. *Mol Biol Cell*. 2015;26:91–103. doi: 10.1091/mbc.E14-06-1073.
10. van De Sluis B, Rothuizen J, Pearson PL, van Oost BA, Wijnenga C. Identification of a new copper metabolism gene by positional cloning in a purebred dog population. *Hum Mol Genet*. 2002;11:165–173.
11. Vonk WI, Bartuzi P, de Bie P, Kloosterhuis N, Wichers CG, Berger R, Haywood S, Klomp LW, Wijnenga C, van de Sluis B. Liver-specific *Commd1* knockout mice are susceptible to hepatic copper accumulation. *PLoS One*. 2011;6:e29183. doi: 10.1371/journal.pone.0029183.
12. Gomez TS, Billadeau DD. A FAM21-containing WASH complex regulates retromer-dependent sorting. *Dev Cell*. 2009;17:699–711. doi: 10.1016/j.devcel.2009.09.009.
13. Seaman MN, Gautreau A, Billadeau DD. Retromer-mediated endosomal protein sorting: all WASHed up! *Trends Cell Biol*. 2013;23:522–528. doi: 10.1016/j.tcb.2013.04.010.
14. Harbour ME, Breusegem SY, Seaman MN. Recruitment of the endosomal WASH complex is mediated by the extended ‘tail’ of Fam21 binding to the retromer protein Vps35. *Biochem J*. 2012;442:209–220. doi: 10.1042/BJ20111761.
15. Burstein E, Hoberg JE, Wilkinson AS, Rumble JM, Csomos RA, Komarck CM, Maine GN, Wilkinson JC, Mayo MW, Duckett CS. COMMD proteins, a novel family of structural and functional homologs of MURR1. *J Biol Chem*. 2005;280:22222–22232. doi: 10.1074/jbc.M501928200.
16. Mallam AL, Marcotte EM. Systems-wide studies uncover commander, a multiprotein complex essential to human development. *Cell Syst*. 2017;4:483–494. doi: 10.1016/j.cels.2017.04.006.
17. van de Sluis B, Muller P, Duran K, Chen A, Groot AJ, Klomp LW, Liu PP, Wijnenga C. Increased activity of hypoxia-inducible factor 1 is associated with early embryonic lethality in *Commd1* null mice. *Mol Cell Biol*. 2007;27:4142–4156.
18. Li H, Koo Y, Mao X, Sifuentes-Dominguez L, Morris LL, Jia D, Miyata N, Faulkner RA, van Deursen JM, Vooijs M, Billadeau DD, van de Sluis B, Cleaver O, Burstein E. Endosomal sorting of Notch receptors through

- COMMD9-dependent pathways modulates Notch signaling. *J Cell Biol.* 2015;211:605–617. doi: 10.1083/jcb.201505108.
19. Bartuzi P, Hofker MH, van de Sluis B. Tuning NF- $\kappa$ B activity: a touch of COMMD proteins. *Biochim Biophys Acta.* 2013;1832:2315–2321. doi: 10.1016/j.bbadis.2013.09.014.
  20. Semenova E, Wang X, Jablonski MM, Levorse J, Tilghman SM. An engineered 800 kilobase deletion of Uchl3 and Lmo7 on mouse chromosome 14 causes defects in viability, postnatal growth and degeneration of muscle and retina. *Hum Mol Genet.* 2003;12:1301–1312.
  21. Starokadomskyy P, Gluck N, Li H, et al. CCDC22 deficiency in humans blunts activation of proinflammatory NF- $\kappa$ B signaling. *J Clin Invest.* 2013;123:2244–2256. doi: 10.1172/JCI66466.
  22. Wan C, Borgeson B, Phanse S, et al. Panorama of ancient meta-zoan macromolecular complexes. *Nature.* 2015;525:339–344. doi: 10.1038/nature14877.
  23. Bligh EG, Dyer WJ. A rapid method of total lipid extraction and purification. *Can J Biochem Physiol.* 1959;37:911–917. doi: 10.1139/c69-099.
  24. Gerdes LU, Gerdes C, Klausen IC, Faergeman O. Generation of analytic plasma lipoprotein profiles using two prepacked superose 6B columns. *Clin Chim Acta.* 1992;205:1–9.
  25. de Bie P, van de Sluis B, Burstein E, Duran KJ, Berger R, Duckett CS, Wijmenga C, Klomp LW. Characterization of COMMD protein-protein interactions in NF- $\kappa$ B signalling. *Biochem J.* 2006;398:63–71. doi: 10.1042/BJ20051664.
  26. Gomez TS, Gorman JA, de Narvajias AA, Koenig AO, Billadeau DD. Trafficking defects in WASH-knockout fibroblasts originate from collapsed endosomal and lysosomal networks. *Mol Biol Cell.* 2012;23:3215–3228. doi: 10.1091/mbc.E12-02-0101.
  27. Pratt JM, Simpson DM, Doherty MK, Rivers J, Gaskell SJ, Beynon RJ. Multiplexed absolute quantification for proteomics using concatenated signature peptides encoded by QconCAT genes. *Nat Protoc.* 2006;1:1029–1043. doi: 10.1038/nprot.2006.129.
  28. Rohlmann A, Gotthardt M, Hammer RE, Herz J. Inducible inactivation of hepatic LRP gene by cre-mediated recombination confirms role of LRP in clearance of chylomicron remnants. *J Clin Invest.* 1998;101:689–695. doi: 10.1172/JCI1240.
  29. Bjørklund MM, Hollensen AK, Hagensen MK, Dagnaes-Hansen F, Christoffersen C, Mikkelsen JG, Bentzon JF. Induction of atherosclerosis in mice and hamsters without germline genetic engineering. *Circ Res.* 2014;114:1684–1689. doi: 10.1161/CIRCRESAHA.114.302937.
  30. van Vlijmen BJ, van den Maagdenberg AM, Gijbels MJ, van der Boom H, HogenEsch H, Frants RR, Hofker MH, Havekes LM. Diet-induced hyperlipoproteinemia and atherosclerosis in apolipoprotein E3-Leiden transgenic mice. *J Clin Invest.* 1994;93:1403–1410. doi: 10.1172/JCI117117.
  31. van Vlijmen BJ, van 't Hof HB, Mol MJ, van der Boom H, van der Zee A, Frants RR, Hofker MH, Havekes LM. Modulation of very low density lipoprotein production and clearance contributes to age- and gender-dependent hyperlipoproteinemia in apolipoprotein E3-Leiden transgenic mice. *J Clin Invest.* 1996;97:1184–1192. doi: 10.1172/JCI118532.
  32. van de Sluis B, Mao X, Zhai Y, Groot AJ, Vermeulen JF, van der Wall E, van Diest PJ, Hofker MH, Wijmenga C, Klomp LW, Cho KR, Fearon ER, Vooijs M, Burstein E. COMMD1 disrupts HIF-1 $\alpha$ /beta dimerization and inhibits human tumor cell invasion. *J Clin Invest.* 2010;120:2119–2130. doi: 10.1172/JCI40583.
  33. Donoso M, Cancino J, Lee J, van Kerkhof P, Retamal C, Bu G, Gonzalez A, Cáceres A, Marzolo MP. Polarized traffic of LRP1 involves AP1B and SNX17 operating on Y-dependent sorting motifs in different pathways. *Mol Biol Cell.* 2009;20:481–497. doi: 10.1091/mbc.E08-08-0805.
  34. McNally KE, Faulkner R, Steinberg F, et al. Retriever is a multiprotein complex for retromer-independent endosomal cargo recycling. *Nat Cell Biol.* 2017;19:1214–1225. doi: 10.1038/ncb3610.
  35. Stockinger W, Sailler B, Strasser V, Recheis B, Fasching D, Kahr L, Schneider WJ, Nimpf J. The PX-domain protein SNX17 interacts with members of the LDL receptor family and modulates endocytosis of the LDL receptor. *EMBO J.* 2002;21:4259–4267.
  36. Farfán P, Lee J, Larios J, Sotelo P, Bu G, Marzolo MP. A sorting nexin 17-binding domain within the LRP1 cytoplasmic tail mediates receptor recycling through the basolateral sorting endosome. *Traffic.* 2013;14:823–838. doi: 10.1111/tra.12076.
  37. Burden JJ, Sun XM, García AB, Soutar AK. Sorting motifs in the intracellular domain of the low density lipoprotein receptor interact with a novel domain of sorting nexin-17. *J Biol Chem.* 2004;279:16237–16245. doi: 10.1074/jbc.M313689200.
  38. Dieckmann M, Dietrich MF, Herz J. Lipoprotein receptors—an evolutionarily ancient multifunctional receptor family. *Biol Chem.* 2010;391:1341–1363. doi: 10.1515/BC.2010.129.
  39. Wang Y, Huang Y, Hobbs HH, Cohen JC. Molecular characterization of proprotein convertase subtilisin/kexin type 9-mediated degradation of the LDLR. *J Lipid Res.* 2012;53:1932–1943. doi: 10.1194/jlr.M028563.
  40. Röhrl C, Stangl H. HDL endocytosis and resecretion. *Biochim Biophys Acta.* 2013;1831:1626–1633. doi: 10.1016/j.bbailip.2013.07.014.